Simple instruments for continuous measurements of trapped particles

P. Bühler (paul.buehler@psi.ch), A. Zehnder (alex.zehnder@psi.ch), L. Desorgher (laurent.desorgher@psi.ch), W. Hajdas (wojtek.hajdas@psi.ch)

Paul Scherrer Institute, CH–5232 Villigen PSI, Switzerland

E. Daly (edaly@wm.estec.esa.nl), L. Adams (ladams@estec.esa.nl)

ESA/ESTEC, NL–2200 AG Noordwijk, The Netherlands

Abstract

In order to keep space radiation environment models up–to–date regular measurements are needed. To measure the high energy particle environment instruments can be used which are small, power saving, and have low weight, to be acceptable as additional payload on any spacecraft. Since two years now a first version of such an instrument is working in space and proves to deliver reliable information on the particle environment. An improved version, the Standard Radiation Environment Monitor, is under development and will be available until the end of 1997.

1. Introduction

High energy particles trapped in the Earth's radiation belts form a particular danger to spacecrafts and their equipment. High energy particles can penetrate deep into a satellite and cause upsets in the electronics or unrecoverable damage [1]. It is therefore of practical importance, not only for design, but also for spacecraft operations, to have models able to predict the particle environment for any position at any time. Up to now static models have been commonly used, constructed from a set of data measured over a particular period, which are supposed to describe average particle fluxes [2],[3]. They do not take into account the dynamics and variability of the environment. The magnetosphere is known to be a dynamical system, strongly influenced by the solar wind and Interplanetary Magnetic Field. It is therefore crucial to consider solar and magnetospheric data simultaneously in constructing forecasting models. Moreover, forecasts must be based on actual data, which allows comparison of prediction and observation, and improvement of the model. This implies that the "system" must be continuously monitored. Whereas solar data is continuously gathered by different ground and space-based observatories, trapped particles are measured only sporadically by instruments covering specific parts of geomagnetic coordinate space. In order to overcome this shortage of particle data, the European Space Agency, ESA is sponsoring the development of a simple instrument for measuring high energy particles, which is light and requires low-power, to be acceptable as a supplementary payload on many scientific and applications satellites. This has the advantage of being low-cost, potentially resulting in many carriers and provides the host spacecraft with valuable radiation environment and effects housekeeping data. The first step in this direction has been the construction of two models of the Radiation Environment Monitor, REM, launched into two different orbits in 1994. It has proved to be a reliable monitor of radiation belt particles. A revised version, the Standard REM, SREM, is being developed and will be available in 1997.

In section 2 we give a brief description of the REM. Examples of in–orbit measurements made with REM in the last two years are discussed in section 3 with special emphasis on the solar influence on the earth's high energy particle environment. In section 4 an introduction to the newly developed SREM is given.

2. The Radiation Environment Monitor

The REM has been built for monitoring the high energy particle environment on spacecrafts. It accumulates energy transfer spectra of charged particles in two silicon detectors and is sensitive to protons in with energies E > 30 MeV and to electrons with energies E > 1 MeV. The energy transfer spectra are accumulated for typically 100 sec and binned into 16 detector channels. The main aperture of the instrument is defined by a cone of $\pm 45°$. However, due to weight restrictions the surrounding shielding has been kept low allowing especially protons to penetrate also from the sides (for a full description of the instrument see Bühler et al. [4]).

A difficulty in building electron detectors is to prevent the count rates to be contaminated with high energy protons. Electrons in the MeV range deposit close to the minimum ionizing energy in silicon (≈ 0.37 keV/μm) – the energy protons with E > 300
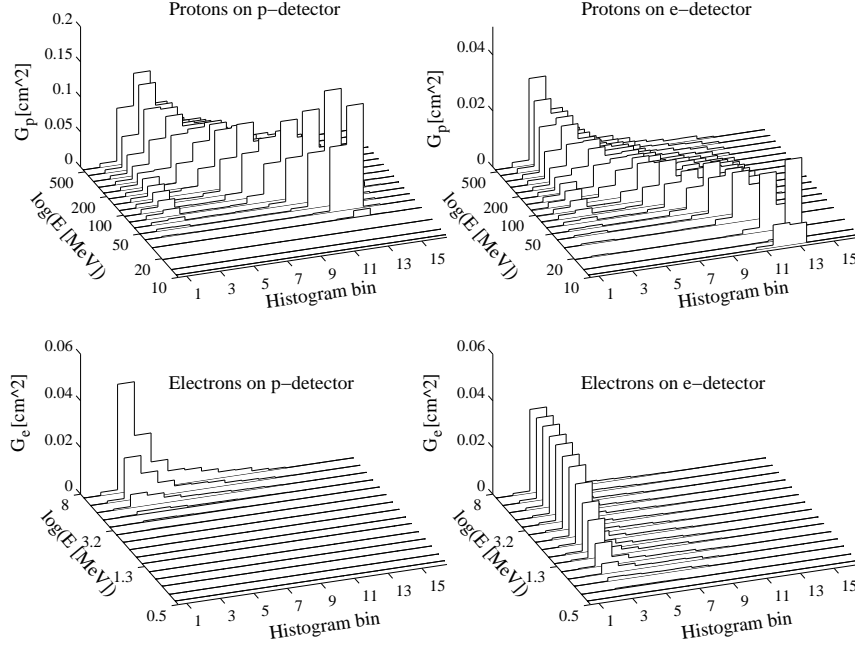
Figure 1: Geometric factors of the REM aboard Mir which have been determined by calibration measurement and extensive numerical simulations.

MeV deposit. Therefore, only from ΔE measurements these particles can not be distinguished. This problem can be solved by using stacks of different detectors and active shielding [5] what however complicates the system.

The idea behind the construction of REM is to accept that electron channels can be contaminated by protons, but to measure the proton flux independently and to use this information to deduce the proton contribution in the electron channels.

Therefore REM consists of two detectors. Each detector uses one silicon diode which is shielded by a spherical dome of a few mm aluminium. One detector is shielded with an additional layer of tantalum which lowers the penetration of MeV electrons considerably, although can not eliminate it totally. However, by using the simultaneous measurements of both detectors, information on the electron and proton fluxes can be gained. An important input for the spectral deconvolution of the measured ΔE histograms are the geometric factors $G_k(E, i)$ which describe the energy response of the detectors. G_k is proportional to the probability that an incident particle of species k, with energy E will be detected and counted in detector channel i. Special efforts have been taken to determine the geometric factors of the REM detectors. The flight instruments have been calibrated with protons and electrons at various energies and in addition extensively numerically simulated, including realistic mass distribution models of

the spacecraft. An example is presented in Figure 1 where the geometric factors of the REM which is flying aboard the Russian space station Mir is shown. Note that there are geometric factors for protons, electrons and both detectors.

3. REM in-orbit measurements

In 1994 two REMs have been brought into different orbits. One with the UK small satellite STRV–1B into a Geostationary Transfer Orbit, GTO (250 km – 36000 km, 7° inclination, 10 h period), and one has been fixed at the outside of the Russian space station Mir, which orbits the earth in a circular Low Earth Orbit, LEO (400 km, 51.6° inclination, 90 min period).

Trapped particle fluxes can be ordered and described in B–L coordinates, where B is the magnetic field strength and L, the L–shell parameter [6]. Figure 2 shows the coverage of the two REM orbits in the B–L plane. The single hatched area is covered by Mir and the cross–hatched area by STRV–1B. The lines running from the upper left to the lower right indicate the location of the mirror points for particles with a particular equatorial pitch angle. Particles with pitch angles larger than the labeled values can not reach regions above the lines. So for example at L=5, only outer belt particles with equatorial pitch angles smaller than $\approx$ 5° can reach Mir – only a small part of the outer belt population.

For a complete description of the environment a large coverage of the B–L plane has to be striven for. In addition, the knowledge of the omnidirectional flux over the whole range of B–values at a given L allows
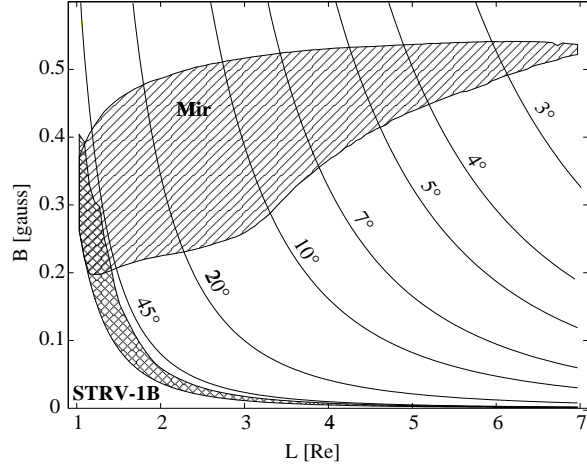

Figure 2: Coverage of B–L plane by STRV–1B and Mir. The solid lines indicate the location of the mirror points for the labeled equatorial pitch angles.

to determine the pitch angle distribution [7].

3.1 Solar influence on the earth's radiation belts

The earth environment is strongly influenced by the solar irradiation, which comprises electromagnetic emission and also particles in the solar wind. This emission undergoes variations, cyclic ones due to the 11–year solar cycle and 27–day solar rotation period, but also non–cyclic ones like solar flares and energetic proton events for example. These variations are reflected in the state of the earth's environment. In the following we will demonstrate with REM measurements the impact of solar radiation on the earth's radiation belts.

Outer belt variations The period of time covered with REM measurements is in the declining phase of the solar 11–year activity cycle. This phase is characterized by decreasing solar magnetic activity which results in a decrease of the EUV and X–ray emission and drop of the number of sporadic events. In the two years since August 1994 only two proton events have been detected by GOES satellites. During solar maximum this number would be typically 20. Due to the lack of eruptive events, the solar wind arriving at the magnetopause is characterized by recurrent fast wind streams which are escaping the sun from coronal holes. The impact of these fast wind streams on the magnetosphere cause strong variations in the high energy electron population trapped in the outer radiation belt. In Figure 3 the 1.2 MeV electron flux measured by REM aboard STRV–1B at L=4.5

is plotted versus time.

Two main features can be noted, the repeated occurrence of rapid depletions and increases with a typical period of 27 days and the absence of strong peaks during winter and summer. The strong periodic variations are associated with the interaction of recurrent fast solar wind streams with the magnetosphere. The arrival of a fast solar wind stream at the earth causes first a depletion of the outer belt high energy electron population within typically one day. This is followed by a rapid (few days) increase where the level reached depends on the wind peak velocity. The phase until the next fast stream arrives is characterized by a slow decay of the measured flux.

The low fluxes during winter and summer are not due to the absence of fast solar wind streams during that time. But although solar wind streams of similar velocity and density impinge upon the magnetosphere their effect on the trapped electrons is different than during spring and fall. The effectiveness of the solar wind – magnetosphere interaction is controlled by the orientation of the earth's magnetic dipole axis with respect to the solar wind flow. For more details on the dynamics of the outer belt electrons see Desorgher et al. [8] in this volume.
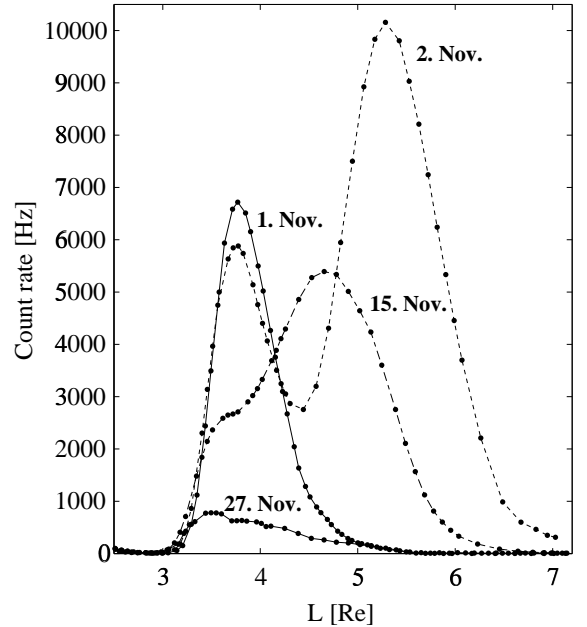

Figure 4: STRV–REM count rates versus L at different times. Not only the total fluxes but also the spatial distribution of the outer belt electrons is variable.

Unlike a geostationary satellite at constant L≈6, like GOES for example, STRV–1B allows to study the radiation belts over a range of L. Not only the total flux varies with time but also the distribution of the electrons in L–space. That the spatial distribution can have various shapes is illustrated in Figure 4 where
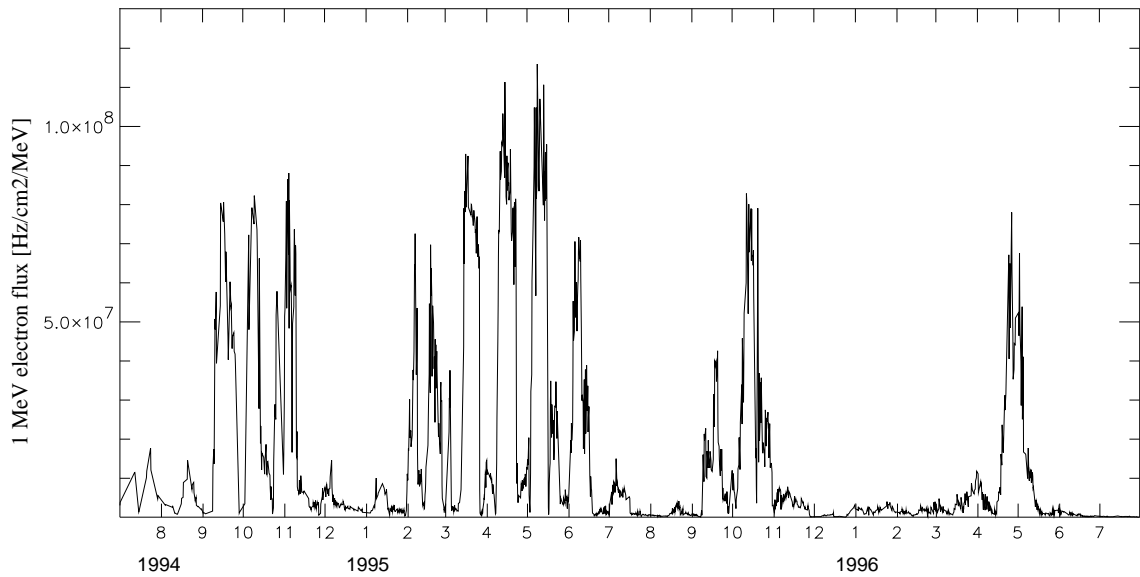
3

Figure 3: 1 MeV electron fluxes measured by REM on STRV–1B at L=4.5 versus time. The large flux peaks are associated with the occurrence of fast solar wind streams impinging on the earth's magnetosphere. The difference between summer/winter and spring/fall can be accounted to by a semiannual varying effectiveness of the solar–wind magnetosphere interaction.

STRV–REM count rate versus L profiles are plotted for 4 different passages through the outer belt in November 1995. On 1 November the electron distribution has a single peak, centered at L≈3.7 (bold line). One day latter on 2 November a new peak has appeared at L≈5.2 which is superposed on the old distribution, resulting in a double peaked distribution (dashed line). In the following the fluxes slowly decayed, drifting towards lower L values.

There are different possibilities to incorporate such new data into environmental models reaching from simple averaging to more sophisticated methods like sorting data by magnetic activity, which can, for example result in models as function of Ap [9], using new data to scale existing static models [10], or use simultaneous solar wind, IMF, and geomagnetic index data to train neural networks [11]. Current data is also needed to test and improve numerical models, aiming to describe the dynamical behaviour of the trapped particles [12].

South Atlantic Anomaly The radiation environment of Mir is dominated by protons in the inner radiation belt. The largest proton fluxes are encountered around L=1.4 at low B values. Due to the specific geometry of the earth's magnetic field, the magnetic field strength B at the Mir altitude has a minimum located above the east cost of Brazil. This region of enhanced radiation is called the South Atlantic Anomaly, SAA. It is also in this region where the protons dip deepest into the earth's atmosphere where they interact with the ambient particles and can get lost. Variations of the atmospheric density

are expected to modulate the loss rate of trapped particles and thus the trapped particles fluxes in the SAA. In Figure 5 the daily average dose measured in the SAA by Mir–REM is plotted versus time.
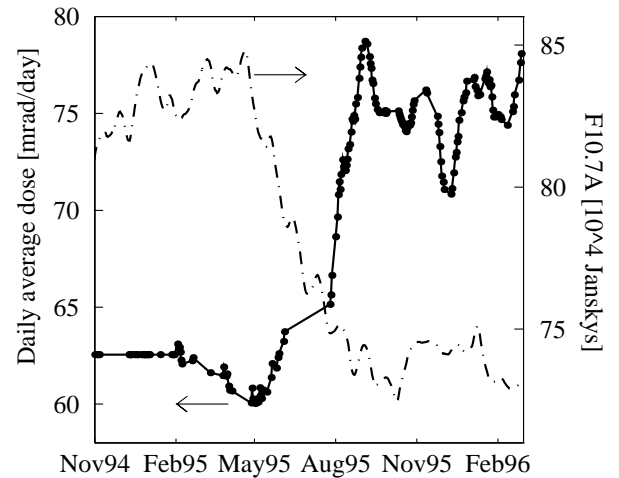

Figure 5: Daily average SAA dose measured by Mir–REM and 10.7 cm solar radio emission versus time. The decrease of F10.7A is accompanied with an increase of the SAA dose.

In the same figure also the three month averaged 10.7 cm solar radio flux, F10.7A is shown. We use here the solar radio emission as measure for the solar EUV and X–ray emission which is responsible for the heating of the upper atmosphere. Around the middle of 1995 the SAA dose increased by 25%. At the same time the solar radio flux decreased by about the

4

same factor. Calculations show that this decrease of heating power causes a lowering of the atmospheric density in the SAA region by typically 20% which could be responsible for the enhanced SAA doses.

The atmosphere is also responsible for an anisotropy of the proton fluxes in the SAA. Due to the fact that the cyclotron motion of protons is clock–wise around the magnetic field lines and the magnetic field in the SAA has a dip angle of $\approx 50°$ and points toward north, the guiding center of particles arriving from the east at the detector is below the point of observation, for particles arriving from the west it is above. Particles coming from east will have experienced denser parts of the atmosphere than those from the west and will be more absorbed. The resulting difference between eastward and westward flowing proton fluxes is called east–west effect [13]. On Mir the REM is shielded from the back by the massive space station. Thus sorting the observations by the orientation of the detectors with respect to the local magnetic field it was possible to measure the east–west effect [14]. In Figure 6 Mir–REM count rates in the high energy proton channels at L=1.4 are plotted as function of B for eastward (asterisks) and westward (dots) orientation of the detectors, respectively. The average ratio between west and east is 4.3. Only recently a model for the anisotropic proton flux has been included in ESA's radiation belt model software UNIRAD [15].
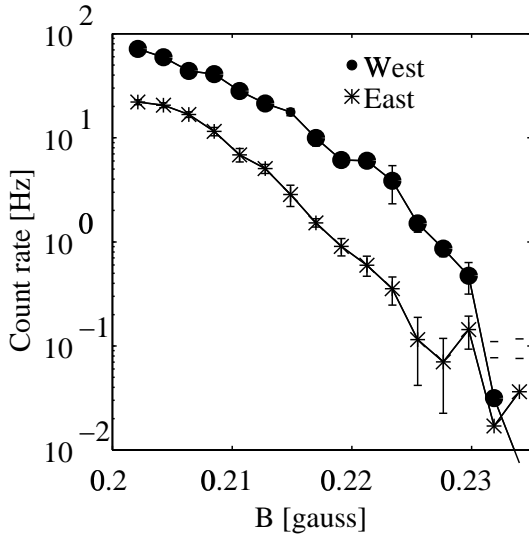
Figure 6: East–west effect measured with Mir–REM at L=1.4. The average count rate ratio between westward and eastward oriented detectors is 4.3.

4. The Standard Radiation Environment Monitor

SREM is an improved version of REM. It consists of two detector systems. A scheme of the two detectors is shown in Figure 7. Detector 3 is a single silicon diode detector. The main entrance window is covered with 0.7 mm aluminium which defines the lower energy threshold for electrons to ≈ 0.3 MeV and for protons to ≈ 10 MeV. Detector 1,2 uses two silicon diodes arranged in a telescope configuration. The main entrance of this detector is covered with 2 mm aluminium. The two diodes are separated by a 1.7 mm thick aluminium and 0.7 mm thick tantalum layer. The advantage of this design compared the the old REM is the fact that the telescope detector Detector 1,2 allows to measure the high energy proton fluxes without electron contamination. The shielding between the two diodes in the telescope prevents the passage of electrons. Protons with energies greater than ≈ 30 MeV however go through. Thus using the two diodes in coincidence gives pure proton count rates which are used to deduce the proton contribution in the electron channels. 15 discriminator levels are available to bin the detected events. Any two of the levels can be used to rise an alarm flag when the count rates exceed a programmable threshold. This alarm signal can then be used to control the operation of the spacecraft and its instruments. The detector electronics is capable of processing a detection rate of 100 kHz. The SREM is contained in one single box of $10 \times 10 \times 20$ cm with a weight of 2.5 kg. The box contains the two detector systems with the analog and digital frontend electronics, a power supply, and a telemetry and telecommand interface which, due to a modular build up, can be adapted to any spacecraft system. The power consumption is 2 W.
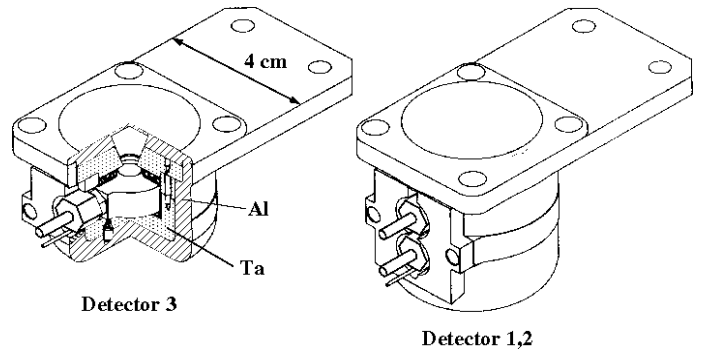
Figure 7: Scheme of the SREM detectors. Detector 3 is a single silicon diode detector, whereas Detector 1,2 is a telescope using two silicon diodes.

SREM is actually build by oerlikon – contraves and will be available until the end of 1997 [16].

5. Conclusion

Amplitude and spatial distribution of the high energy particle fluxes in the magnetosphere are highly variable and strongly linked to solar activity. In order to make reliable predictions of the environ-

ment encountered by satellites, regular measurements are needed which allow to keep models up-to-date. Valuable data can be gained with instruments which are small, light (2.5 kg) and power saving (2 W) and therefore acceptable as supplementary payload on many satellites. Build-in alarm functions which can be used by the host spacecraft to control operation during encounters of high particle fluxes gives such an instrument an additional practical meaning. Using low-resource demanding instruments as standard equipment on a number of satellites would allow to gather valuable data, saving the costs for extra launches.

Acknowledgement

References

[1] Daly, E. The evaluation of space radiation environment for ESA projects. *ESA Journal*, 12:229, 1988.

[2] Vette, J.I. The AE-8 trapped electron model environment. Technical report, NSSDC WDC-A-R&S 91-24, NASA-GSFC, 1991.

[3] Sawyer, D.M. and Vette, J.I. AP-8 trapped proton environment for solar maximum and solar minimum. Technical report, NSSDC WDC-A-R&S 76-06, NASA-GSFC, 1976.

[4] Bühler, P., Ljungfelt, S., Mchedlishvili, A., Schlumpf, N., Zehnder, A., Adams, L., Daly, E., Nickson, R. Radiation Environment Monitor. *Nucl. Instr. and Meth. in Phys. Res. A*, 368:825, 1996.

[5] Dichter, B.K., Hanser, F.A., Sellers, B., Hunerwalder, J.L. High energy electron fluxmeter. *IEEE Trans. Nucl. Sci.*, 40(2):252, 1993.

[6] McIlwain, C.E. Coordinates for mapping the distribution of magnetically trapped particles. *Journal of Geophysical Research*, 66:3681, 1961.

[7] Badhwar, G.D. and Konradi, A. Conversion of omnidirectional proton fluxes into a pitch angle distribution. *J. Spacecraft and Roc.*, 27(3):350, 1990.

[8] Desorgher, L., Bühler, P., Zehnder, A., Adams, L., Daly, E. Variations of the outer radiation belt during the last two years. In *ESA Symposium on Environment modelling for space-based applications*, Noordwijk, The Netherlands, September 1996, in press.

[9] Brautigam, D.H., Bell, J.T. CRRESELE documentation. Technical Report PL-TR-95-2128, Phillips Laboratory, Hanscom AFB, MA 01731-3010, July 1995.

[10] Friedel, R. A Dynamic Data-Driven Radiation Belt Model Based on CRRES Data. In *ESA Symposium on Environment modelling for space-based applications*, Noordwijk, The Netherlands, September 1996, in press.

[11] G.A. Stringer, I. Heuten, C. Salazar and B. Stokes. Artificial Neural Network (ANN) Forecasting of Energetic Electrons at Geosynchronous Orbit. In *Workshop on Radiation Belts: Models & Standards*, Brussels, October 1995, in press.

[12] Boscher, D., Bourdarie, S., Beutier, T. Dynamic modeling of trapped particles. *IEEE Trans. Nucl. Sci.*, 43(2):416, 1996.

[13] Heckman, H.H. and Nakano, G.H. East-West asymmetry in the flux of mirroring geomagnetically trapped protons. *Journal of Geophysical Research*, 68(8):2117, 1963.

[14] Bühler, P., Desorgher, L., Zehnder, A., Adams, L., Daly. REM measurements aboard Mir during 1995. In *COSPAR Scientific meeting*, Birmingham, United Kingdom, July 1996, in press.

[15] Kruglanski, M. Trapped proton anisotropy at low altitudes. TREND, Technical note 6, Belgian Institute for Space Aeronomy, April 1996.

[16] oerlikon – contraves space, Marketing & Sales Department, CH – 8052 Zürich.